LPV Detection Filter Design for a Boeing 747-100/200 Aircraft

István Szászi*

Budapest University of Technology and Economics, Hungary

Andrés Marcos,† and Gary J. Balas‡

University of Minnesota, Minneapolis, Minnesota 55455

József Bokor §

Computer and Automation Research Institute, Hungary

Abstract

This paper presents a fault detection and isolation (FDI) filter design using a linear parameter varying (LPV) model of the longitudinal dynamics of a Boeing 747 series 100/200. The LPV FDI filter design is based on an extension of the fundamental problem of residual generation concepts elaborated for linear, time-invariant systems. Typically, the FDI filters are designed for open–loop model, and applied in closed–loop. This paper shows an application of a LPV FDI filter for actuator failure detection and isolation in the closed–loop longitudinal LPV system and to the full nonlinear Boeing 747 aircraft simulation which represents the "true" system.

*PhD Student, Department of Control and Transport Automation, e-mail: szaszi@kaut.kka.bme.hu

†Graduate Student, Department of Aerospace Eng. and Mechanics, e-mail: marcosa@aem.umn.edu

‡Professor, Dept. of Aerospace Eng. and Mechanics, e-mail: balas@aem.umn.edu, corresponding author.

§Professor, Hungarian Academy of Sciences, e-mail: bokor@sztaki.hu

1 Nomenclature

$\bar{c}$	wing chord, meter
c_7	$= \frac{1}{I_{yy}}$, inertia coefficient, $kg^{-1}m^{-2}$
$\bar{q}$	dynamic pressure, N/m^2
S	reference surface area, m^2
z_{eng}	engine position z-axis, m
Tn	trust force, Newton
α	angle of attack (AoA), radians
α_w	wing design plane, $\alpha_w = \alpha\frac{180}{pi} + 2$ deg
s_α, c_α	sine, cosine of AoA, rad

2 Introduction

Modern control systems and algorithms are becoming increasingly complex and sophisticated. Consequently, the issue of availability, reliability, operating safety are of major importance. These issues are especially important for safety critical systems such as nuclear reactors, cars and aircraft flight control systems. For safety critical systems, the consequence of faults can be extremely serious in terms of human mortality and environmental impact. Therefore, there is a growing need for on-line supervision and fault diagnosis to increase the reliability of safety critical systems.

A traditional approach to fault diagnosis in the wider application context is based on hardware redundancy methods which use multiple sensors, actuators, computers and software to measure and control a particular variable. In analytical redundancy schemes, the resulting difference generated from the consistency checking of different variables is called as a residual signal. The residual should be zero when the system is normal, and should diverge from zero when a fault occurs in the system. This zero and non-zero property of the residual is used to determine whether or not faults have occurred. Analytical redundancy makes use of a mathematical model and the goal is the determination of faults of a system from the comparison of available system mea-

surements with a priori information represented by the mathematical model, through generation of residual quantities and their analysis.

There are various approaches to residual generation for, see *e.g.* the parity space approach [1], the multiple model method, detection filter design using geometric approach [2] or on frequency domain concepts [3] unknown input observer concept (Chapter 3, [4]) and dynamic inversion based detection [5]. Most of the design approaches refer to linear, time-invariant (LTI) systems, but references to nonlinear cases can be found in reference [4].

The geometric approach to the design detection filters was initiated by Massoumnia for LTI systems [2] and was applied by Bokor *at al.*, to LTV systems in reference [6]. These concepts have been used to build a linear parameter–varying (LPV) fault detection and isolation (FDI) design procedure in in references [7, 8]. Related results on FDI filter design based in the geometric approach appeared recently for bilinear systems, see Hammouri et.al. [9] while Persis and Isidori considered input affine nonlinear systems [10, 11].

Aircraft models are usually nonlinear and time varying. One approach to flight control is to derive a family of linear models based on linearization around given setpoints and synthesize a flight controller that is gain scheduled through out the flight envelope. A more efficient and theoretically sound approach is to rewrite the models into linear parameter varying (LPV) or quasi LPV (qLPV) models that have an LTI or LTV form:

$$\begin{aligned} \dot{x}(t) &= A(\rho)x(t) + B(\rho)u(t) + \sum_{j=1}^{m} L_j(\rho)v_j(t) \\ y(t) &= Cx(t), \end{aligned} \tag{1}$$

where x is the state variable and $\rho(t) = [\rho_1(t), \dots, \rho_N(t)]^T]$ is a known function up to time t. It is assumed that each parameter ρ_i ranges between known extremal values $\rho_i(t) \in [-\overline{\rho}_i, \overline{\rho}_i]$. This parameter set will be denoted by $\mathcal{P}$. The case when the ρ_i functions depend on the state(s) of the system or its components is called quasi-LPV (qLPV).

The fault models appear linearly in the LPV model, equation (1): their direction is

given by $L_j(\rho)$ and the failures to be detected are modeled by the unknown functions $v_j(t)$.

It is worth noting that all input affine nonlinear models can be rewritten in qLPV form and very effective control system design methods have been developed for LPV and qLPV systems [12, 13, 14]. These methods have been successfully applied to various aerospace control applications [15, 16, 17].

If the control system is designed for this model class, it is reasonable to design FDI algorithms and possible reconfiguration design strategies for LPV and qLPV systems. Since these models are basically time varying or nonlinear, use of time domain FDI design approaches based on geometric concepts are well suited as a solution. This is the approach investigated in this paper with development of an actuator fault detection and isolation system for a Boeing 747 aircraft.

The detection filter design method will be described for LPV and qLPV systems where the state space matrices depend affinely on the parameters:

$$A(\rho) = A_0 + \rho_1 A_1 + \cdots + \rho_N A_N, \tag{2}$$

$$B(\rho) = B_0 + \rho_1 B_1 + \cdots + \rho_N B_N, \tag{3}$$

$$L_j(\rho) = L_{j,0} + \rho_1 L_{j,1} + \cdots + \rho_N L_{j,N}. \tag{4}$$

The contribution of this paper is the first application of LPV FDI filtering to a full nonlinear aicraft model. The complete FDI design process, including an example, and experiences on the LPV FDI filter design and its application to the closed-loop aircraft system are presented. The paper is organized as follows. Section 3 provides a very quick review of the fundamental problem of residual generation for LTI systems. Following this, the geometric concepts needed to elaborate the design procedure are discussed for the above class of LPV systems. In section 4, the nonlinear and LPV model for the longitudinal motion of the Boeing 747 are presented. The LTI controller used is briefly described in section 5. Section 6 shows the fault detection results using LPV detection filters applied to the closed-loop simulation of the Boeing 747 LPV model and a LTI controller. This is followed by the application of the LPV FDI filter

to the full nonlinear Boeing 747 model. Section 7 provides some concluding remarks.

3 Fundamental problem of residual generation for LTI and LPV systems

Let us consider the following LTI system, that has two failure events.

$$\begin{aligned} \dot{x}(t) &= Ax(t) + Bu(t) + L_1 v_1(t) + L_2 v_2(t) \\ y(t) &= Cx(t). \end{aligned} \tag{5}$$

In equation (5), $x(t) \in \mathcal{X}$ is the state variable, $u(t) \in \mathcal{U}$ is the known control input, $y(t) \in \mathcal{Y}$ is the known output, the arbitrary time-varying functions $v_i(t) \in \mathcal{L}_i$ are the unknown failure modes. The term $L_1 v_1(t)$ represents the faulty behavior of the actuator that we are trying to monitor, i.e., a nonzero $v_1(t)$ should show up in the output of the residual generator $r(t)$. Similarly, $L_2 v_2(t)$ represents the faulty behavior of the other actuator which should not affect $r(t)$. The task of designing a residual generator that is sensitive to L_1 and insensitive to L_2 is called the fundamental problem of residual generation (FPRG) [18].

Let us denote by $\mathcal{S}^*$ the smallest unobservability subspace (UOS) containing $\mathcal{L}_2$, where $\mathcal{L}_2 = \mathrm{Im} L_2$. $\mathcal{S}^*$ is the largest UOS in $\mathrm{Ker} C$ containing $\mathcal{L}_2$.

The $\mathcal{S}^*$ can be computed by the UnObservability Subspace Algorithm *UOSA* [19]:

$$\mathcal{S}_0 = \mathcal{X} \tag{6}$$

$$\mathcal{S}_k = \mathcal{W}^* + (A^{-1}\mathcal{S}_{k-1}) \cap \mathrm{Ker} C, \tag{7}$$

where $\mathcal{W}^*$ is the minimal (C,A)-invariant subspace containing $\mathcal{L}_2$. As it is well known, for LTI models, a subspace $\mathcal{W}$ is (C,A)-invariant if $A(\mathcal{W} \cap \mathrm{Ker} C) \subseteq \mathcal{W}$ that is equivalent with the existence of a matrix D such that $(A + DC)\mathcal{W} \subseteq \mathcal{W}$.

Proposition 1. *FPRG has a solution if and only if* $\mathcal{S}^* \cap \mathcal{L}_1 = 0$, *moreover, if the problem has a solution, the dynamics of the residual generator can be assigned arbitrary.*

The equation $\mathcal{S}^* \cap \mathcal{L}_1 = 0$ indicates that v_2 should not affect the output of the residual generator $r(t)$.

It can be proved, e.g. [2], that the residual generator has the form

$$\begin{aligned} \dot{w}(t) &= Nw(t) - Gy(t) + Fu(t) \\ r(t) &= Mw(t) - Hy(t), \end{aligned} \tag{8}$$

where H is a solution of $\mathrm{Ker}HC = \mathrm{Ker}C + \mathcal{S}^*$, and M is a unique solution of $MP = HC$, where P is the projection $P : \mathcal{X} \to \mathcal{X}/\mathcal{S}^*$.

In order to obtain the matrices in equation (8), consider D_0 such that $(A + D_0C)\mathcal{S}^* \subseteq \mathcal{S}^*$ (i.e. D_0 makes $\mathcal{S}^*$ a (C, A) invariant subspace) , and denote by $A_0 = A + D_0C|_{\mathcal{X}/\mathcal{S}^*}$. By construction, the pair (M, A_0) is observable, hence there exists a D_1 such that the poles of $N = A_0 + D_1M$ can be assigned arbitrary. Then set $G = PD_0 + D_1H$ and $F = PB$.

Note that the important step in the design of the filter is to assign the image of the second failure signature L_2 to the unobservable subspace of the residual $r(t)$. Also the necessary condition simply states that the image of the first failure signature L_1 should not intersect with the unobservable subspace of the residual generator to ensure that the failure of the first actuator shows up in the residual r.

FPRG results can be extended to the case of multiple events. This has a solution if and only if $\mathcal{S}_i^* \cap \mathcal{L}_i = 0$, where $\mathcal{S}_i^*$ is the smallest unobservability subspace containing $\bar{\mathcal{L}}_i = \sum_{j \neq i} \mathcal{L}_j$. For the case of multiple faults, a bank of filters are designed such that each one of them is sensitive to a particular fault and completely unsensitive to the others. This provides a complete isolation of the fault effects from each other.

These results can be extended to the parameter varying case. In order to derive the filter synthesis procedure it is necessary to generalize the notions of invariant subspaces, (C,A)-invariant and unobservability subspaces to the parameter varying situation. Introduce the definition of *parameter varying (C,A)-invariant subspaces*, as follows:

Definition 1. *Let $\mathcal{C}(\rho)$ denote Ker $C(\rho)$. Then a subspace $\mathcal{W}$ is called a parameter varying (C,A)-invariant subspace if for all the parameters $\rho \in \mathcal{P}$:*

$$A(\rho)(\mathcal{W} \cap \mathcal{C}(\rho)) \subseteq \mathcal{W}. \tag{9}$$

As in the classical case one has the following characterization of the parameter varying (C,A)-invariant subspaces:[8]

Proposition 2. *$\mathcal{W}$ is a parameter varying (C,A)-invariant subspace if and only if for any $\rho \in \mathcal{P}$ there exists a state feedback matrix $D(\rho)$ such that*

$$(A(\rho) + D(\rho)C(\rho))\mathcal{W} \subseteq \mathcal{W}. \tag{10}$$

The set of all parameter varying (C,A)-invariant subspaces containing a given subspace $\mathcal{B}$ admits a minimum denoted by

$$\mathcal{W}^*(\mathcal{B}) := \min \mathcal{W}(C(\rho), A(\rho), \mathcal{B}). \tag{11}$$

The notion of "unobservability subspace" extends to LPV systems as the largest subspace such that there exist a parameter dependent gain matrix $D(\rho)$ and constant output mixing map H such that

$$(A(\rho) + D(\rho)C)\mathcal{S} \subseteq \mathcal{S}, \text{ for all } \rho \in \mathcal{P}, \tag{12}$$

$$\mathcal{S} \subseteq \text{Ker}HC. \tag{13}$$

For the LPV systems defined in equation (1), one can obtain the following algorithms [8].

Proposition 3. *The minimal parameter varying (C,A)-invariant subspace containing a given subspace $\mathcal{L}$ can be computed as follows.*

$$PVCAISA: \quad \mathcal{W}^0 = \mathcal{L}$$
$$\mathcal{W}^{k+1} = \mathcal{L} + \sum_{l=0}^{N} A_l(\mathcal{W}^k \cap Ker\ C), \quad k \geq 0.$$

The minimal parameter varying unobservability subspace containing a given subspace $\mathcal{W}^*$ can be computed as

$$PVUOSA: \quad \mathcal{S}^0 = \mathcal{W}^* + Ker\ C$$
$$\mathcal{S}^{k+1} = \mathcal{W}^* + (\cap_{l=0}^{N} A_l^{-1}\mathcal{S}^k) \cap Ker\ C \qquad k \geq 0.$$

Let us recall the fact, see [2, 9], that there exist matrices H, $D(\rho)$ such that $\mathcal{S}^*$ is a parameter varying $(HC, A(\rho) + D(\rho)C)$-invariant subspace. Moreover, if one starts with a minimal subspace $\mathcal{W}^*$, given by PVCAISA presented above, then KerHC = $\mathcal{W}^*$ + Ker$C$ and $D(\rho)$ is determined by $\mathcal{W}^*$.

Using the above concepts, it is possible to extend the synthesis of residual generators to LPV systems. For simplicity, assume that the number of faults is equal to 2 in Proposition 4.

Proposition 4. *For LPV systems (1) one can design a residual generator of type*

$$\dot{w}(t) = N(\rho)w(t) - G(\rho)y(t) + F(\rho)u(t) \tag{14}$$
$$r(t) = Mw(t) - Hy(t), \tag{15}$$

if and only if the smallest (parameter varying) unobservability subspace $\mathcal{S}^*$ containing $\mathcal{L}_2$ has $\mathcal{S}^* \cap \mathcal{L}_1 = 0$, where $\mathcal{L}_1 = \sum_{j=0}^{N} ImL_{1,j}$.

An outline of computation for matrices of a LPV filter is as follows. Let H be the solution of KerHC = $KerC + \mathcal{S}^*$, and M the unique solution of $MP = HC$, where P is the projection $P : \mathcal{X} \to \mathcal{X}/\mathcal{S}^*$. By the definition of the unobservability subspaces there is a matrix $D_0(\rho)$ such that $(A(\rho) + D_0(\rho)C)\mathcal{S}^* \subseteq \mathcal{S}^*$ holds. Then set

$A_0(\rho) = A(\rho) + D_0(\rho)C|_{\mathcal{X}/\mathcal{S}^*}$, and $F = PB(\rho)$.

In order to obtain a quadratically stable residual generator one can set $N(\rho) = A_0(\rho) + D_1(\rho)M$ in (14), where $D_1(\rho) = D_{10} + \rho_1 D_{11} + \cdots \rho_N D_{1N}$ is determined such that the Linear Matrix Inequality (LMI) defined as,

$$(A_0(\rho) + D_1(\rho)M)^T X + X(A_0(\rho) + D_1(\rho)M) < 0 \tag{16}$$

holds for all the vertices of the parameter space with a suitable $D_1(\rho)$ and $X = X^T > 0$ [7]. The steps of the above design procedure are discussed in detail for a simple academic example in the Appendix.

4 Longitudinal LPV model of Boeing 747-100/200

The FDI filter design is focused on the longitudinal axis of a Boeing 747 series 100/200 aircraft and it requires an LPV model of the aircraft. The longitudinal LPV model is obtained from a high-fidelity nonlinear model of a Boeing 747 series 100/200 aircraft. The Boeing 747-100/200 aircraft is an intercontinental wide-body transport with four fan jet engines designed to operate from international airports. The nonlinear model for the Boeing 747-100/200 aircraft was obtained from references [20, 21].

The body-axes longitudinal motion of the Boeing 747, not including flexible effects, can be described by the differential equations (assuming no wind components):

$$\dot{\alpha} = \frac{[-F_x \cdot s_\alpha + F_z \cdot c_\alpha]}{m \cdot V_T} + q \tag{17}$$

$$\dot{q} = c_7 \cdot M_y \tag{18}$$

$$\dot{\theta} = q \tag{19}$$

$$\dot{V}_T = \frac{1}{m}\left[F_x \cdot c_\alpha + F_z \cdot s_\alpha\right] \tag{20}$$

$$\dot{h}_e = V_T \cdot c_\alpha \cdot s_\theta - V_T \cdot s_\alpha \cdot c_\theta = V_T \cdot s_\gamma \tag{21}$$

The states of the system are angle of attack, α (rad), pitch rate, q (rad/s), pitch angle, θ (rad), true airspeed, V_T (m/s), and altitude, h_e (m). Longitudinal control

is performed through a movable horizontal stabilizer, δ_{st} (rad), with four embedded elevator segments and by thrust from the four engines, Tn_i (Newtons). Pitch trim is provided mainly by the horizontal stabilizer. Under normal operation the inboard and outboard elevators move together, $\delta_e = \delta_{E_I} = \delta_{E_O}$ (deg) and for the purpose of this research it is assumed that the four elevator segments move and fail together.

The body-axes aerodynamic forces and moments are given by

$$F_x = -\bar{q}S \cdot [C_D \cdot c_\alpha - C_L \cdot s_\alpha] + \sum_{i=1}^{4} Tn_i - mg \cdot s_\theta \tag{22}$$

$$F_z = -\bar{q}S \cdot [C_D \cdot s_\alpha + C_L \cdot c_\alpha] \tag{23}$$

$$- 0.0436 \cdot \sum_{i=1}^{4} Tn_i + mg \cdot c_\theta \tag{24}$$

$$M_y = \bar{q}S\bar{c} \cdot \left\{ C_m - \frac{1}{\bar{c}} \left[(C_D \cdot s_\alpha + C_L \cdot c_\alpha)\bar{x}_{cg} - (C_D \cdot c_\alpha - C_L \cdot s_\alpha)\bar{z}_{cg} \right] + \frac{\bar{c}\dot{\alpha}}{V_T} \left[C_{m_{\dot{\alpha}}} - \frac{\bar{x}_{cg}}{\bar{c}} \cdot C_{L_{\dot{\alpha}}} \cdot c_\alpha \right] \right\} + \sum_{i=1}^{4} Tn_i \cdot z_{eng_i}. \tag{25}$$

where $\bar{c}$ (meters) is the wing chord, $c_7 = 1/I_{yy}$ $(kg^{-1}m^{-2})$ is an inertial coefficient, $\bar{q}$ (N/m^2) is dynamic pressure, S (m^2) is reference surface area, z_{eng} (m) is z-axis engine position, $\bar{x}_{cg}$ and $\bar{z}_{cg}$ (m) are center of gravity position, $m \cdot g$ (Newtons) is the aircraft weight, and s_α, c_α (radians) are the sine and cosine of the angle of attack respectively.

In reference [21], the longitudinal nonlinear model of the Boeing 747-100/200 is simplified by reducing the complexity of the aerodynamic coefficients. The simplified model maintains a high degree of accuracy and all the important nonlinear characteristics of the full set of aerodynamic coefficients. This simplification of the nonlinear model was performed to facilitate the LPV modeling task.

The LPV model developed for FDI filter design is non-standard in the sense that for control design the number of scheduling variables are usually kept small (since the computational requirement for controller synthesis increases with the number of

scheduling variables). In the present case, i.e. LPV FDI design based on FPRG concepts, it is important for the LPV model to be affine in the scheduling variables (and of course linear in the states and control inputs vectors) and also to be an accurate representation of the nonlinear model it represents to avoid model uncertainty. There are several theoretical issues of importance related to the LPV modeling stage in the FDI approach proposed: e.g. persistence of excitation and linear independency of the scheduling variables, but these are open questions outside the scope of this paper. The engineering solution found to address the linear condition was to introduce a fictitious input set always to 1 radian which multiplies those terms from the equations of motion that could not be rewritten as linear combinations of any of the states or existing control inputs. In order to provide with an LPV model which is a good approximation to the nonlinear model the number of scheduling variables was significantly increased, up to 9 parameters. See Appendix B for an example of a nonlinear state transformation into the affine LPV model format.

The states of the LPV model are the same as the nonlinear longitudinal model. The output measurements are angle of attack α, pitch rate q, true velocity V_T, pitch angle, θ, and altitude, h_e. The inputs are elevon deflection δ_e, stabilizer deflection δ_{st}, throttle Tn and an ideal fictitious input, δ_{fic}, assumed to be always equal to 1 radians. The LPV model used for LPV filter design depends affinely on nine scheduling parameters, ρ. The general form of the LPV model is given by equation (1) where the system matrices are given by $A(\rho) \in \mathcal{R}^{5\times 5}$ and $B(\rho) \in \mathcal{R}^{4\times 4}$ and $N = 9$.

The scheduling variables to be used in the LPV model are the following: $\rho = \big[\bar{q},\ \frac{\bar{q}}{V_t},\ \frac{1}{V_T},\ \gamma,\ C_{L_{basic}}\cdot\frac{\bar{q}}{V_T},\ \frac{\partial C_L}{\partial \delta_{el}}\cdot\frac{\bar{q}}{V_T},\ C_{D_{Mach}}\cdot\bar{q},\ \frac{\partial C_m}{\partial \delta_{el}}\cdot\bar{q},\ C_{m_{basic}}\cdot\bar{q}\big]^T$. This set of scheduling variables is formed by combining aircraft stability derivatives and physical variables (i.e dynamic pressure, $\bar{q}$, true airspeed, V_T, and flight path angle, γ radians). The term $C_{L_{basic}}(\alpha_w, M)$ is the basic lift coefficient for the rigid airplane at the zero stabilizer angle in free air with the landing gear retracted, $\frac{\partial C_L}{\partial \delta_{el}}(h_e, M)$ is the change in basic lift coefficient due to change in elevator, $C_{D_{Mach}}(M, C_L^*)$ is the Mach effect on drag coefficient, $\frac{\partial C_m}{\partial \delta_{el}}(h_e, M)$ is the change in basic pitching moment coefficient due to change in elevator, $C_{m_{basic}}(\alpha_w, M)$ is the basic pitching moment coefficient for the

rigid airplane at the zero stabilizer angle in free air with the landing gear retracted. All the scheduling variables depend nonlinearly, through look-up tables, on altitude, h_e, wing angle of attack, α_w, defined as $\alpha_w = \alpha \cdot \frac{180}{\pi} + 2$ deg and true airspeed, V_T. The flight envelope described by the LPV model is based on these three parameters: $h_e \in [\ 3000\ ,\ 12000\ ]$ meters, $\alpha \in [\ -2\ ,\ 10\ ] \cdot \frac{\pi}{180}$ radians, and $V_T \in [\ 80\ ,\ 300\ ]$ m/sec which covers the Up-and-Away flight envelope used in references [20, 21] (see Table 1 in Appendix B for the scheduling variables limits). The scheduling variables should be measurable parameters and although it could be argued that for a real implementation some of the proposed parameters are not physically accessible it is always possible to use the look-up table descriptions and the available measurements of the altitude, angle of attack and velocity to calculate these scheduling variables.

In order to validate the LPV model, open-loop time responses are obtained and compared to the transient response of the nonlinear model. Specifically, tests are performed to analyze and compare the short-period and phugoid characteristics of the models. Figure 1 shows open-loop time responses of the nonlinear system and the LPV model to an elevator pulse of 6 degrees for 4 seconds. The simulation time is 100 seconds. In order to provide with the correct thrust to excite the phugoid mode an engine model is included in the open-loop simulation. The engine model transforms Engine Pressure Ratio (EPR) command inputs into thrust, Tn, based on the true airspeed measurement. The trim flight condition used in this simulation is straight-level flight with: angle of attack $\alpha = 0.0209$ radians, true airspeed $V_T = 241$ m/s, altitude of $h_e = 9000$ m, $q = 0$ rad/s and $\theta = \alpha$ (i.e. flight path angle $\gamma = 0$ rad). This flight condition results in trim command inputs for the nonlinear model of EPR $= 0.021$ radians, $Tn = 39439$ newtons, $\delta_e = 0.0348$ rad, and $\delta_{st} = -0.0094$ rad. The engine pressure ratio and stabilizer deflection commands are held constant at the previous trim values during the open-loop simulation.

The phugoid or long-period mode is characterized by gradual changes in pitch angle, altitude and velocity over long periods of time, these are clearly shown in the corresponding graphs in Figure 1. The short-period dynamics are more important and are characterized for a short period oscillation heavily damped affecting mainly angle

of attack and pitch rate [22]. The LPV model is an almost perfect approximation to the nonlinear model short period as there are no discernible differences in the corresponding graphs in Figure 1. Additional flight conditions and manoeuvres were tested yielding similar results. They are not included for lack of space.

5 Boeing 747-100/200 Longitudinal LTI Controller

For closed-loop simulations, an LTI $\mathcal{H}_\infty$ controller synthesized at the same equilibrium point at which the aircraft model is trimmed is obtained. In the subsequent closed-loop simulations the equilibrium point used to design the controller and initialized the models is given by an altitude of 7000 m and a true airspeed of 241 m/s. This section provides a brief description of the LTI control synthesis based on the controller presented in reference [23].

In the aforementioned reference, a reconfigurable LPV controller for the longitudinal motion of the Boeing 747-100/200 is presented. The LPV controller has the particularity of scheduling on true airspeed, altitude, and the elevator fault signal produced by an FDI filter. The basis of the reconfiguration is to use an alternative control surface in the case the elevator surfaces suffer a malfunction. The alternative control is provided by the horizontal stabilizer, which results in a loss in performance (i.e. there is a reduced speed of response for the flight path angle). The details are given in reference [23]. In this application, only the architecture and weights given in the previous reference are used to obtain an LTI $\mathcal{H}_\infty$-controller without implementing any LPV or reconfigurable strategy (i.e. we assume a no-fault case synthesis). This means that faults are not considered directly in the synthesis of the controller but the controller should be robust enough to handle non-critical faults.

The controller objectives are to achieve de-coupled tracking of flight-path angle command γ_c and velocity command V_c with settling times of 15 sec and 45 sec respectively with the elevator surface fully functional, and the rejection of gust disturbances

for the Up-and-Away flight envelope. Figure 2 shows the controller architecture. The corresponding weights: performance W_p, uncertainty W_u, command scaling W_{scl}, noise W_n, ideal models T_{id}, and engine, elevator, and stabilizer dynamic models are given in the aforementioned reference.

The controller has five measurements available: flight path angle γ (rad), acceleration $\dot{V}$ ($\mathrm{m/s^2}/g$), pitch angle θ (rad), pitch rate q (rad/s), and velocity V (m/s). Note that these inputs are different to those from the plant, the latter are manipulated before being fed to the controller. There are two control outputs: elevator deflection δ_{e_c} (rad), and thrust Tn_c (N). It was mentioned before that the plant inputs included the two controller outputs and a stabilizer input, δ_{st} (rad). The latter is used for trim purposes and is held constant at the corresponding trim value for the entire simulation when implemented with the FDI filter. These controller outputs and stabilizer input are passed through first order actuators before going to the plant: the elevator actuator dynamics are given by $act_e = \dfrac{27}{s+27}$ and the engine dynamics and stabilizer actuator by $act_{Tn} = act_{st} = \dfrac{1}{2s+1}$.

6 FDI filter design using LPV model

This section deals with the design, simulation, and analysis of a fault detection LPV filter used to detect elevator and thrust faults for the longitudinal motion of the Boeing 747-100/200. The filter approach relies on open-loop LPV models of the aircraft, see section 4. Realistically these filters are implemented in closed-loop, hence simulations are performed with the LTI $\mathcal{H}_\infty$ controller and the nonlinear model to ensure its validity. From theoretical results, see references [24, 25], it is known that when there is no model uncertainty the filter in closed-loop can be obtained by multiplying the open-loop filter by the inverse of the sensitivity function (i.e. $F_{closed} = F_{open} \cdot S^{-1}$). The open-loop and closed-loop designs can be said to be equivalent on the nominal case. This fact relies on the existence of a separation principle between the controller and the filter for the non-uncertainty case, i.e. the information for the filter synthesis in the nominal case is not affected by the closed-loop inclusion of the controller. In the

uncertain case this separation principle does not exist, i.e the uncertainty is introduced to the filter through controller feedback, factually decreasing the amount of information the filter gets. A possible approach to compensate for this decrease of information is to design an integrated controller and filter, e.g. the two-parameter controller of reference [26]. Our rationale is to synthesize the filter in the open-loop setting with the assumption that most current systems already have a controller implemented.

The closed-loop simulation set-up is shown in Figure 3. It consists of a LTI $\mathcal{H}_\infty$ controller, the nonlinear plant (or the LPV model) and the FDI filters (one for elevator actuator fault detection and the second for thrust fault detection). The sensors are considered ideal, i.e. y_s equals the outputs of the plant.

The LPV FDI filters designed for the longitudinal motion of the Boeing 747/100-200 aircraft are sensitive to elevator and throttle failure. The LPV FDI filters inputs are the aircraft outputs $(\alpha, q, V_T, \theta, h_e)$ and the actuator outputs $(\delta_e, \delta_{st}, Tn)$. The output of each detection filter is a diagnostic signals known as residual: one for the elevator fault, res_e, and the other for the thrust fault, res_{Tn}, respectively. The LPV model including elevator and throttle failure can be described as:

$$\begin{aligned} \dot{x}(t) &= A(\rho)x(t) + B(\rho)u(t) + L_{el}(\rho)v_{el}(t) + L_T v_T(t) \\ y(t) &= Cx(t), \end{aligned} \tag{26}$$

where

$$A(\rho) = A_0 + \rho_1 A_1 + \cdots + \rho_9 A_9, \tag{27}$$

$$B(\rho) = B_0 + \rho_1 B_1 + \cdots + \rho_9 B_9, \tag{28}$$

$$L_{el}(\rho) = \rho_1 b_{el,1} + \rho_6 b_{el,6} + \rho_8 b_{el,8}, \tag{29}$$

$$L_T = b_{T,0}. \tag{30}$$

The elevator failure signature is parameter dependent since the direction of the elevator depends on parameters. The direction of the throttle failure does not depend on parameters. The b_{el} is that column of B matrix, which represents the elevator

actuator direction and b_T is the column of B matrix associated to throttle direction. The FDI filter is tested during an aircraft maneuver. The γ command used in the simulations is a square wave, starting at 25 sec and ending at 100 sec and the velocity command is a step signal starting at time = 30 sec as seen in Figure 4. The fault scenarios applied in the elevator channel and in the throttle channel and the commands can be seen in the residual plots of Figure 5. The failures are modeled as an additive term in equation (26) corresponding to a loss in effectiveness of the control input channels. This means that the actuator effectiveness has been reduced to a constant value. In case of failures, the actuators are assumed to be able to work when faults have occurred. Although the actuator losses its effectiveness, the aircraft motion can be controlled with increased control action.

The simulation results of the LPV FDI filter for the case of the closed–loop with the LPV model is shown in Figure 4. It is observed that the controller guarantees the tracking performance despite of the fault. Even though the command decoupling objective is achieved, the impact of the faults affect the responses of the controller. Figure 5 shows the control inputs and the outputs of the FDI filters. The first residual, δ_{el} residual, detects the elevator fault while the second diagnostic signal, the Tn residual, is the throttle fault residual. The effect of the failures is decoupled and the residuals give an exact estimation of elevator and throttle fault. The impact of the flight path angle command on the residuals is negligible.

Next, the situation is studied when the FDI filter is applied to the nonlinear longitudinal model which represents the "true" system. Figure 6 shows the simulation results of the LPV FDI filter for the case of the closed–loop nonlinear system. The residual outputs for the nonlinear simulation are shown in Figure 7.

The fault scenarios are the same as before. The effect of the failures is decoupled and the FDI filters tell us the magnitude of the failures and also at what time the failures have occurred in the system. In the case of the nonlinear Boeing 747 aircraft closed-loop the fault estimation error is larger than for the LPV model case. Moreover, there are transients at 25 sec and at 100 sec in the elevator fault residual. The reason for these transients is that the LPV FDI filter is simulated using square wave γ command:

during climbing mode the trim conditions are changing hence this results in a transient signal at the residual outputs. This result is a function of the difference between the LPV and nonlinear model which is illustrated best in the θ variable at 20 seconds into the simulation in Figures 4 and 6. However, when the γ command goes back to zero indicating that the aircraft has reached its commanded altitude and the trim conditions do not change any longer, the fault residuals of FDI filter show only the effective faults. Unfortunately, if the trim conditions change in a long time duration, e.g. when we use a long γ command for take off, then a transient fault signal may appear for an extended period of time. Therefore, knowledge of the trim value would need to be account for in the current formulation of the LPV FDI filter to reduce the potential for false alarms.

7 Conclusion

In this paper, a LPV FDI filter design based on extension of the fundamental problem of residual generation concepts elaborated for LTI systems has been presented through the application of LPV longitudinal model of Boeing 747-100/200. The LPV FDI filter used in this paper is sensitive for elevator and throttle failure. The LPV FDI filter is designed for an open-loop LPV model of the aircraft and is applied to the full nonlinear Boeing 747 closed-loop aircraft. In case of nonlinear closed-loop simulation, the impact of the flight path angle command appears in the residuals as transients, but this does not destroy the reliable operation of the LPV detection filter. For steady state trim conditions the LPV FDI filter performs very well, accurately isolating as well as estimating the magnitude of the faults.

8 Acknowledgments

This research was supported in part by NASA Langley, NASA Cooperative Agreement No. NCC-1-337, Dr. Christine M. Belcastro technical monitor, and in part by the Hungarian National Science Foundation (OTKA) under Grant T-030182.

References

[1] Gertler, J., *Fault Detection and Diagnosis in Engineering Systems*, Marcel Dekker, New York, 1998.

[2] Massoumnia, M.A, "Geometric Approach to the Synthesis of Failure Detection Filters," *IEEE Transactions on Automatic Control*, Vol. 31, No. 9, 1986, pp. 839–846.

[3] Frank, P.M. and Ding, X., "Frequency Domain Approach to Optimally Robust Residual Generation and Evaluation for Model-based Fault Diagnosis," *Automatica*, Vol. 30, No. 5, 1994, pp. 789–804.

[4] Chen, J. and Patton, R.J., *Robust Model-Based Fault Diagnosis for Dynamic Systems*, Kluwer Academic Publishers, 1999.

[5] Szigeti, F., Vera, C.E., Bokor, J., and Edelmayer, A., "Inversion Based Fault Detection and Isolation," *IEEE Proceeding of the Conference on Decision and Control*, Vol. 2, Orlando, FL, December 2001, pp. 1005–1010.

[6] Edelmayer, A., Bokor, J., Szigeti, F., and Keviczky, L, "Robust detection filter design in the presence of time-varying system perturbations," *Automatica*, Vol. 33, No. 3, 1997, pp. 471–475.

[7] Balas, G.J. and Bokor, J., "Detection Filter Design for LPV Systems," *Proceedings of the 4th IFAC Safeprocess 2000 Symposium*, Vol. 2, Budapest, Hungary, June 2000, pp. 653–656.

[8] Balas, G.J., Bokor, J., and Szabó Z., "Failure Detection for LPV Systems - a Geometric Approach," *Proceedings of the American Control Conference*, Vol. 6, Anchorage, AK, May 2002, pp. 4421 –4426.

[9] Hammouri, H., Kinnaert, M., and El Zaagoubi, E. H., "Observer Based Approach to Fault Detection and Isolation for Nonlinear Systems," *IEEE Transactions on Automatic Control*, Vol. 44, No. 10, 1999, pp. 1879–1884.

[10] Persis, C. and Isidori, A., "On the Observability Co-Distributions of a Nonlinear System," *Systems and Control Letters*, Vol. 40, 2000, pp. 297–304.

[11] De Persis, C. and Isidori, A., "A Geometric Approach to Nonlinear Fault Detection and Isolation," *IEEE Transactions on Automatic Control*, Vol. 45, No. 6, June 2001, pp. 853 –865.

[12] Packard, A., "Gain Scheduling via Linear Fractional Transformations," *Systems and Control Letters*, Vol. 22, No. 2, 1994, pp. 79–92.

[13] Becker, G. and Packard, A, "Robust Performance of Linear Parametrically Varying Systems Using Parametrically Dependent Linear Dynamic Feedback," *Systems and Control Letters*, Vol. 23, No. 3, 1994, pp. 205–215.

[14] Apkarian, P. and Gahinet, P., "A Convex Characterization of Gain-Scheduled H_∞ Controllers," *IEEE Transactions on Automatic Control*, Vol. 40, No. 5, May 1995, pp. 853–864.

[15] Balas, G.J., "Linear, Parameter-Varying Control and its Application to a Turbofan Engine," *International Journal of Robust and Nonlinear Control*, Vol. 12, No. 9, July 2002, pp. 763–796.

[16] Fiahlo,I., Balas, G.J., Packard, A., Renfrow, J., and Mullaney, C., "Gain-Scheduled Lateral Control of the F-14 Aircraft During Powered Approach Landing," *Journal of Guidance, Control, and Dynamics*, Vol. 23, No. 3, 2002, pp. 450–458.

[17] Fialho, I. and Balas, G.J., "Road adaptive active suspension design using linear parameter-varying gain-scheduling," *IEEE Transactions on Control Systems Technology*, Vol. 10, No. 1, January 2002, pp. 43–54.

[18] Massoumnia, M.A., *A Geometric Approach to Failure Detection and Identification in Linear Systems*, Ph.D. thesis, Department of Aeronautics and Astronautics MIT, February 1986.

[19] Wonham, W.M., *Linear Multivariable Control: A Geometric Approach*, New York, Springer-Verlag, 1985.

[20] Marcos, A., *A Linear Parameter Varying Model of the Boeing 747-100/200 Longitudinal Motion*, Master's thesis, Department of Aerospace and Engineering Mechanics, University of Minnesota, 2001.

[21] Marcos, A. and Balas, G.J., "Linear Parameter Varying Modeling of the Boeing 747-100/200 Longitudinal Motion," *AIAA 2001 Guidance, Navigation, and Control Conference, AIAA-01-4347*, Montreal, Canada, August 2001.

[22] Nelson, R., *Flight Stability and Automatic Control*, WCB McGraw-Hill, 1998.

[23] Ganguli, S., Marcos, A., and Balas, G.J., "Reconfigurable LPV Control Design for Boeing 747-100/200 Longitudinal Axis," *Proceedings of the American Control Conference*, Vol. 5, Anchorage, AK, May 2002, pp. 3612 –3617.

[24] Niemann, H. and Stoustrup, J., "Robust Fault Detection in Open vs. Closed Loop," *Proceedings of 36th IEEE Conference on Decision and Control*, San Diego, California, Dec. 1997, pp. 4496–4497.

[25] Stoustrup, J. and Grimble, M.J., "Integration Control and Fault Diagnosis: A Separation Result," *Proceedings of IFAC Safeprocess 97, August 1997, Hull, UK*, Aug. 1997.

[26] Stoustrup, J., Grimble, M.J., and Niemann, H., "Design of Integrated Systems for the Control and Detection of Actuator/Sensor Faults," *Sensor Review*, Vol. 17 (2), July 1997, pp. 138–149.

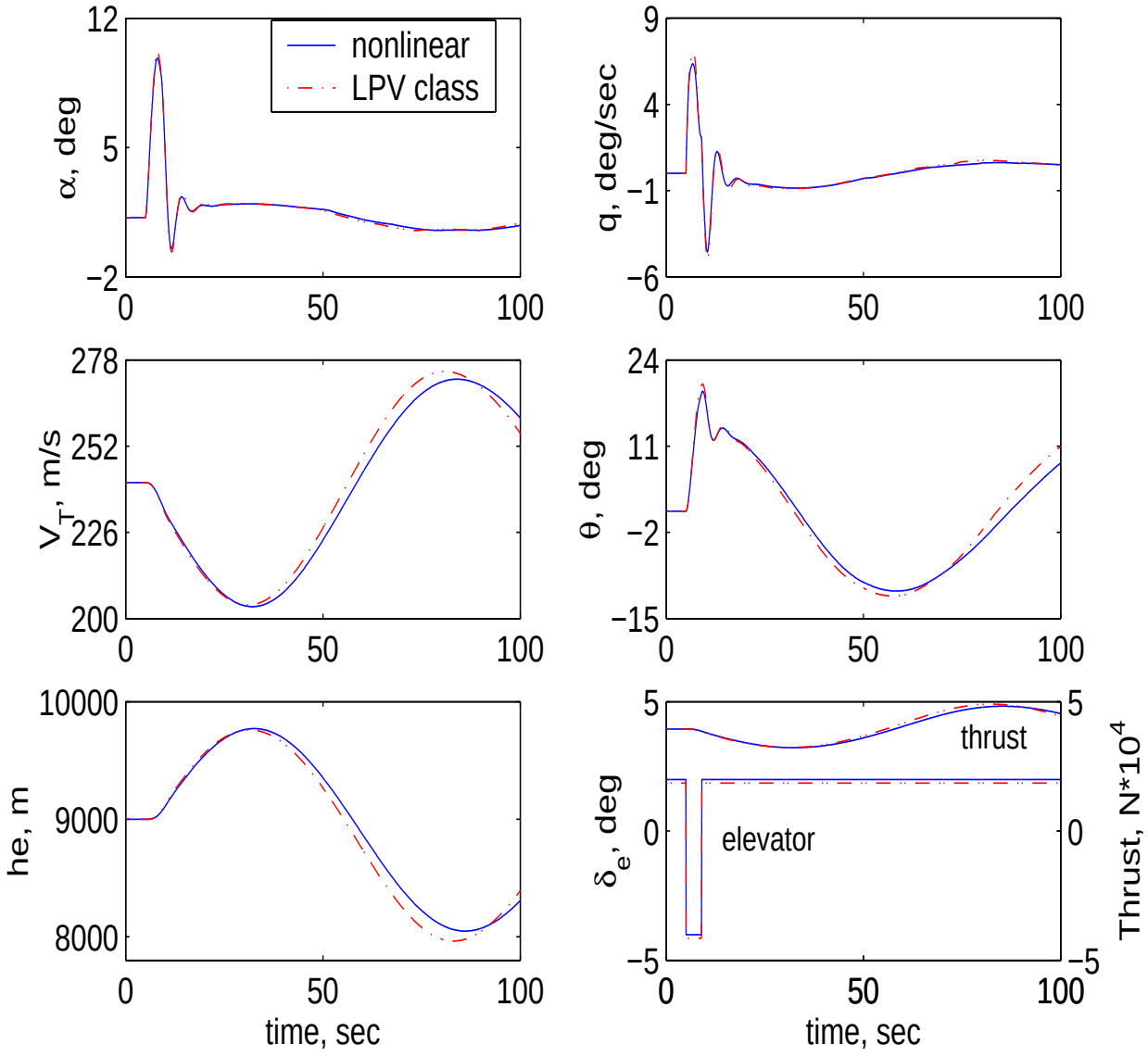

Figure 1: Time responses of LPV and nonlinear models

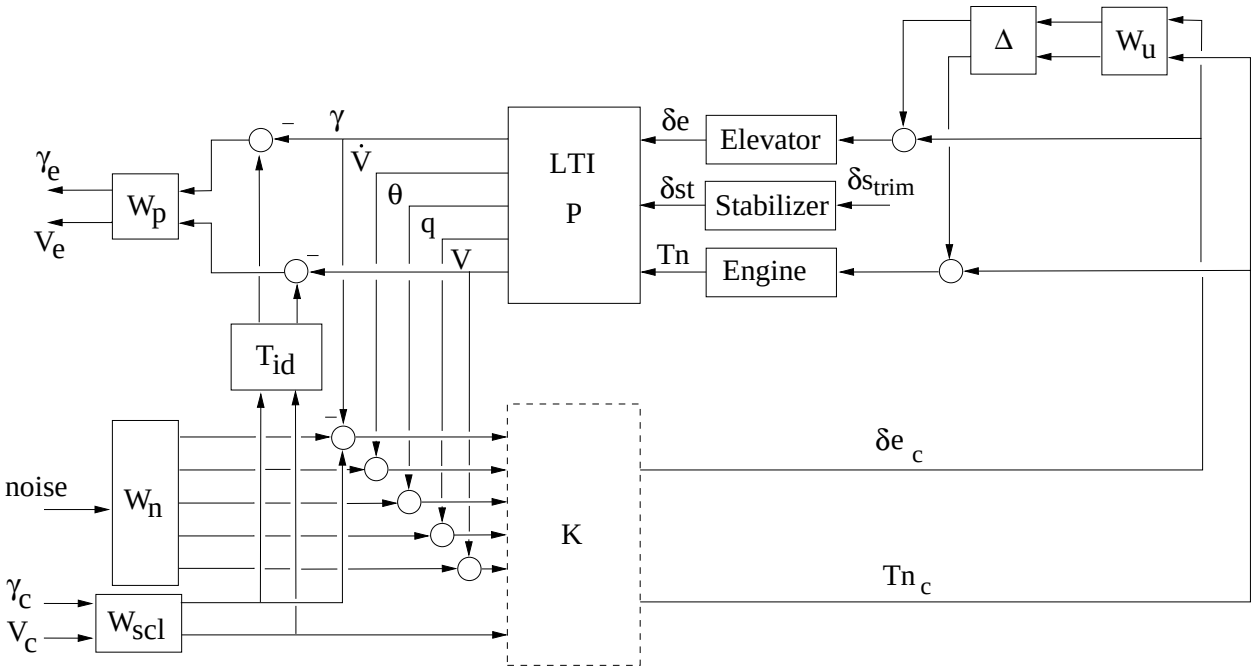

Figure 2: $\mathcal{H}_\infty$ LTI controller interconnection.

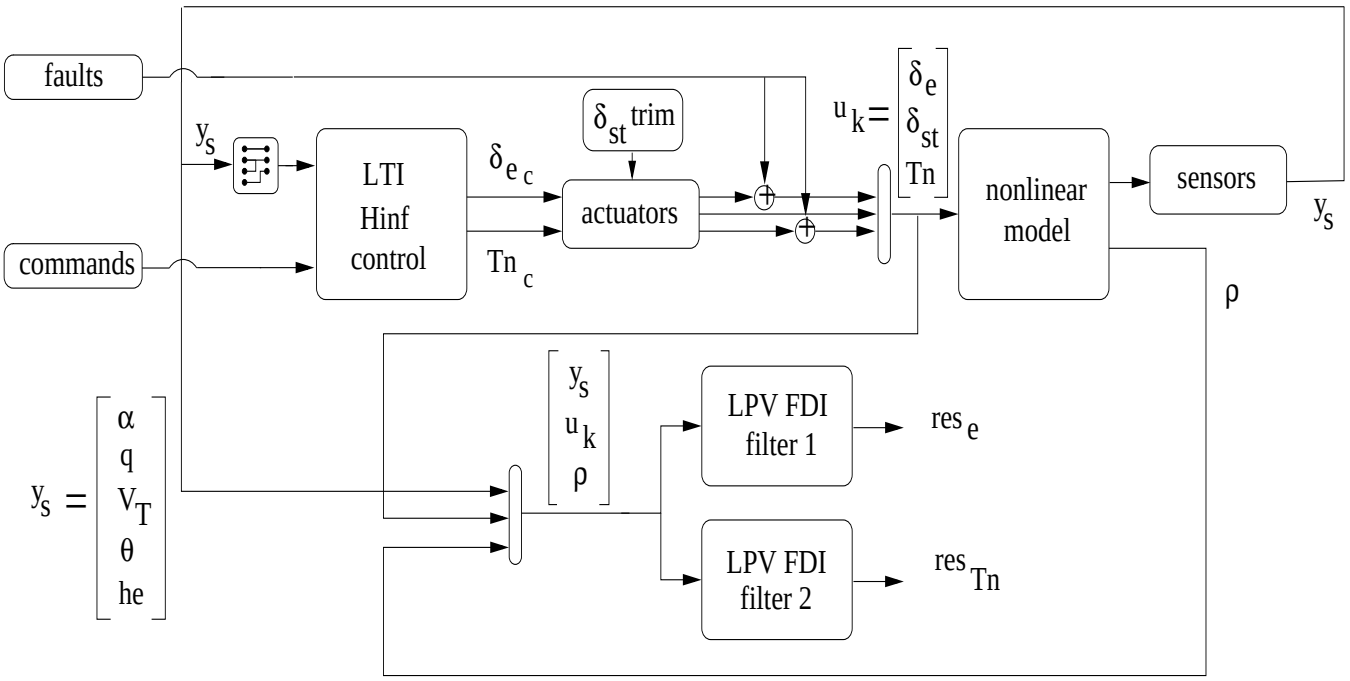

Figure 3: Closed-loop implementation

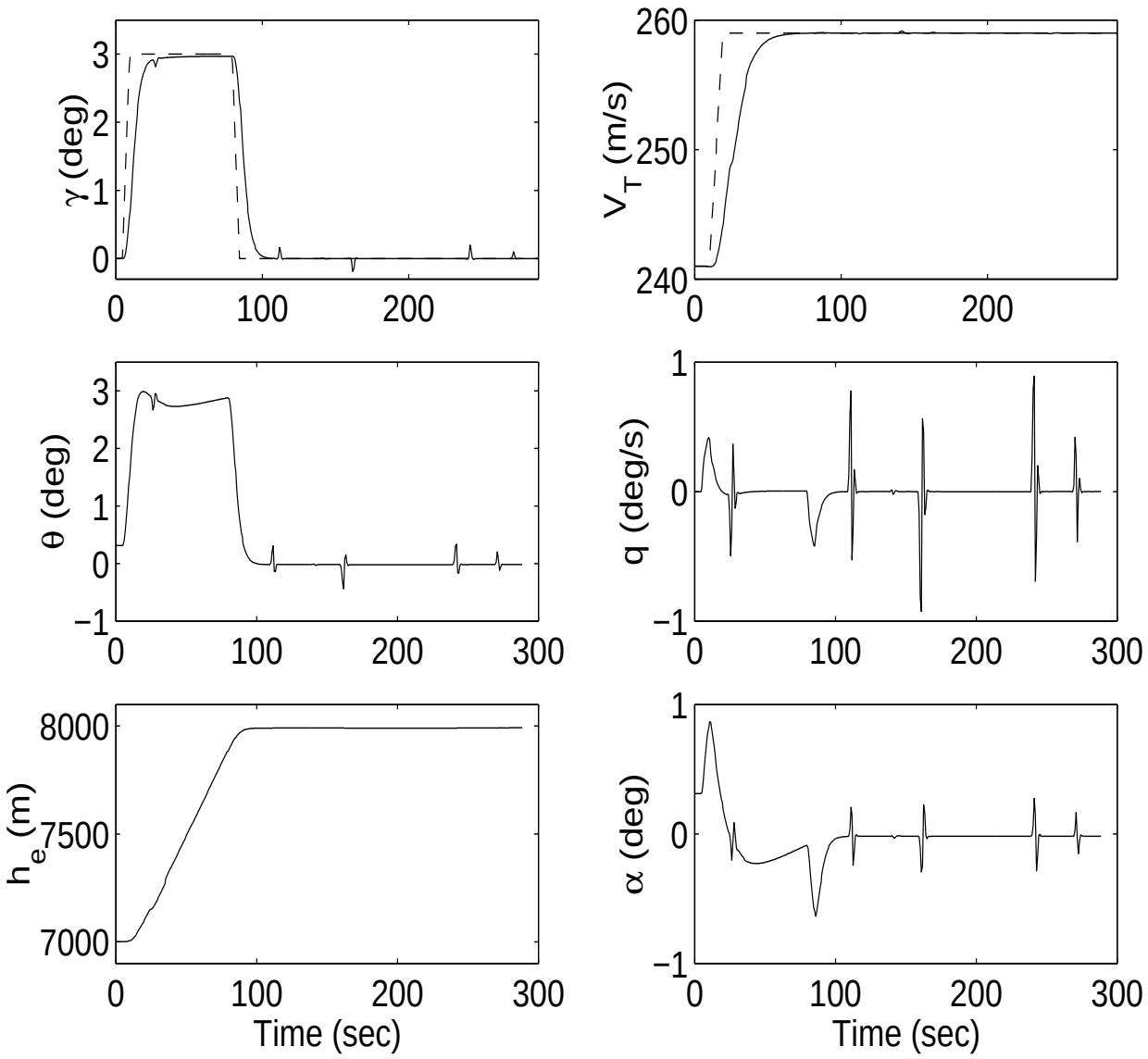

Figure 4: Time responses, LPV model with faults: command (dashed), responses (solid).

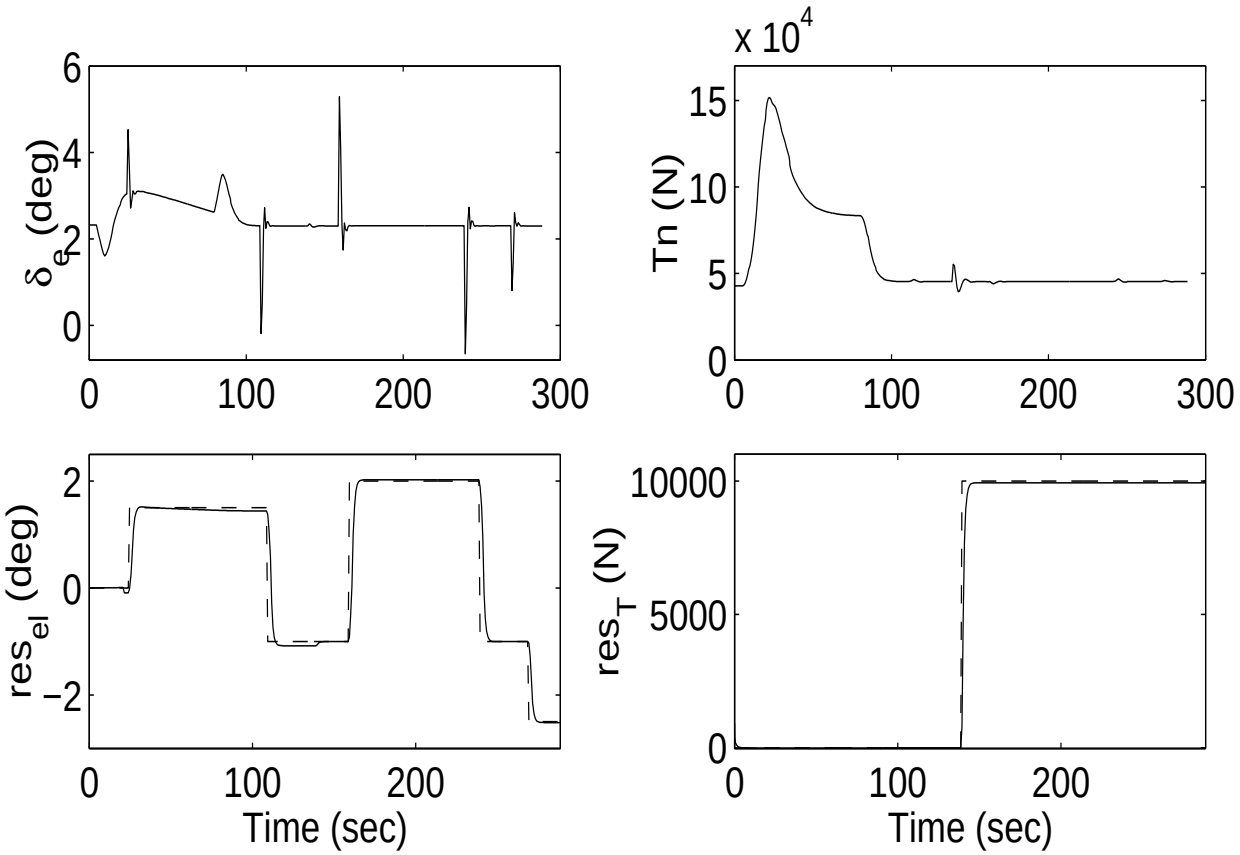

Figure 5: Controller and FDI filter outputs, LPV model: fault (dashed), residual (solid).

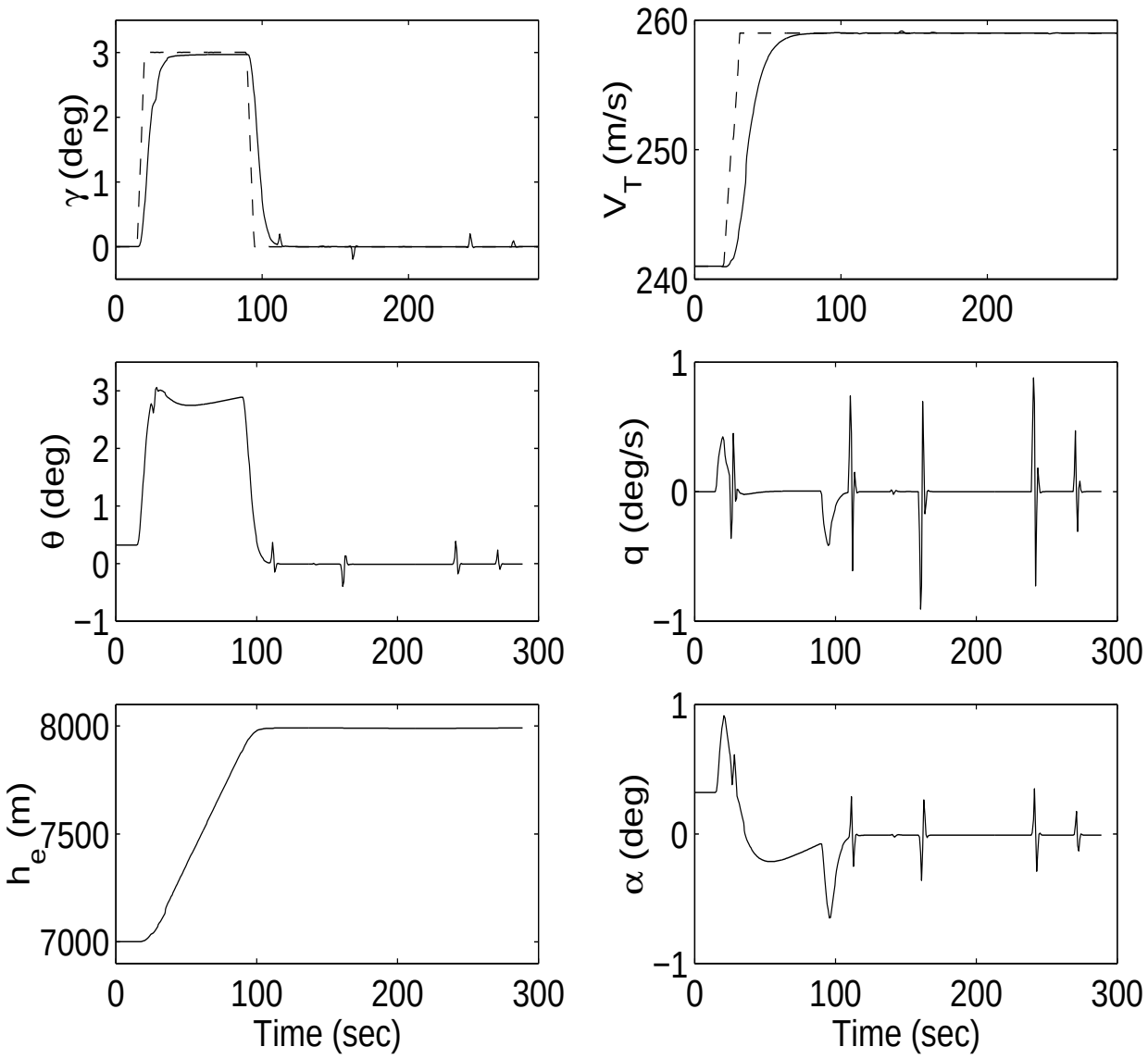

Figure 6: Time responses, nonlinear model with faults: commands (dashed), responses (solid).

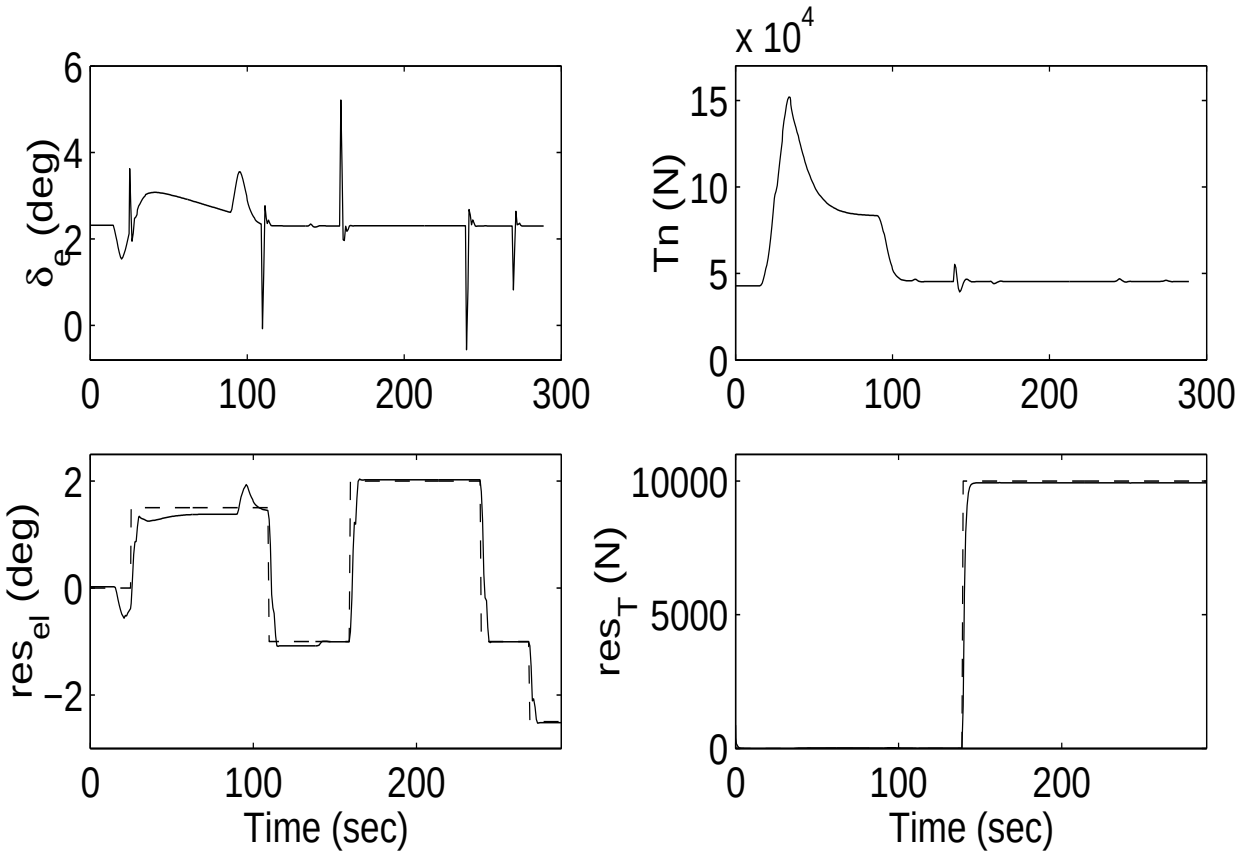

Figure 7: Controller and FDI filter outputs, nonlinear model: fault (dashed), residual (solid).

A Appendix

We consider a simple example in which the matrices are given by

$$A(\rho) = A_0 + \rho(t)A_1 = \begin{bmatrix} \lambda & 0 & 0 \\ 0 & -\nu & \omega \\ 0 & \omega & -\nu \end{bmatrix} + \rho \begin{bmatrix} 0 & 0 & 0 \\ 0 & 1 & 0 \\ 0 & 1 & 0 \end{bmatrix};$$
$$B = \ L = \ [L_1 \ L_2] = \begin{bmatrix} 1 & 0 \\ 0 & 1 \\ 0 & 0 \end{bmatrix}; \qquad C = \begin{bmatrix} 1 & 0 & 0 \\ 0 & 1 & 0 \end{bmatrix}; \tag{31}$$

Given A, B, C, L_1, and L_2 (in the present example we use $\lambda = -2$, $\nu = 1$ and $\omega = 0.5$) the design process goes as follows. The subspaces $\mathcal{W}_i^*$ and $\mathcal{S}_i^*$, containing $\mathcal{L}_i$ (with $i = 1, 2$) are determined first using CAISA and UOSA, respectively.

Since $KerC = \text{span}[0\ 0\ 1]^T$ and $\mathcal{L}_1, \mathcal{L}_2$ are not in $KerC$, using CAISA one immediately obtains that $\mathcal{W}_i^* = \mathcal{L}_i$, $i = 1, 2$. Computation of the unobservability subspace $\mathcal{S}_2^*$ is as follows (the details for computing $\mathcal{S}_1^*$ are identical). Using UOSA we get:

$$\mathcal{S}_2 = \mathcal{W}_2^* + (A_0^{-1}\mathcal{W}_2^* \cap KerC) \cap (A_1^{-1}\mathcal{W}_2^* \cap KerC). \tag{32}$$

It can be seen that one has to compute subspace additions, intersections and inverse images. The latter can be computed using the following result:

Proposition 1. *Let $A : \mathbb{R}^n \to \mathbb{R}^n$, $\mathcal{X} \subset \mathbb{R}^n$ and Im $X = \mathcal{X}$, then*

$$A^{-1}\mathcal{X} = Ker\ X^{\perp}A \tag{33}$$

where $X^{\perp}$ is a maximal solution (a solution with maximum rank) of $X^{\perp}X = 0$.

Let $W = [0\ 1\ 0]^T$, then for a matrix satisfying $W^{\perp}A_0 = 0$ we get $W^{\perp} = \begin{bmatrix} 1 & 0 & 0 \\ 0 & 0 & 1 \end{bmatrix}$ resulting in $(A_0^{-1}\mathcal{W}_2^* \cap KerC) = \text{span}[0\ 1\ \ -.5]^T$ and $(A_0^{-1}\mathcal{W}_2^* \cap KerC) = KerC$.

Using similar arguments one can conclude that $(A_1^{-1}\mathcal{W}_2^* \cap KerC) = KerC$ and $\mathcal{S}_2^* = \mathcal{W}_2^* + KerC$, i.e.

$$\mathcal{S}_2^* = \text{span}\begin{bmatrix} 0 & 0 \\ 1 & 0 \\ 0 & 1 \end{bmatrix}. \tag{34}$$

Simple calculation shows that $\mathcal{S}_1^* = \mathcal{W}_1^* = \text{span}[1\ 0\ 0]^T$.

Having the minimal parameter varying unobservability subspaces containing L_2 we factorize the state space with this $\mathcal{S}_2^*$ subspace and only look at the factor space to prevent any effect of L_2 on the observation of L_1. This is done by a P_i projection matrix, whose kernel is the $\mathcal{S}_i^*$ subspace. Choosing a basis in $\mathcal{S}_i^{*\perp}$ and considering the basis vectors as rows we can get suitable P_i matrices:

$$P_1 = \begin{bmatrix} 0 & 1 & 0 \\ 0 & 0 & 1 \end{bmatrix}, \quad P_2 = [1 \quad 0 \quad 0]. \tag{35}$$

The next step is to compute the gains $D_0^1(\rho),\ D_0^2(\rho)$ that make $\mathcal{S}_1^*,\ \mathcal{S}_2^*$, respectively (C, A)-invariant:

$$(A(\rho) + D_0^i(\rho)C)\mathcal{S}_i^* \subset \mathcal{S}_i^* \quad i = 1, 2. \tag{36}$$

$$\text{where} \qquad D_0^i(\rho) = D_{00}^i + \rho D_{01}^i \tag{37}$$

Denote by S_i the matrix with columns forming a basis of $\mathcal{S}_i^*$. Then using the above formulae we get $S_i^{\perp}(A_j + D_{0j}^i C) = 0,\ i = 1, 2,\ j = 0, 1.$

In the example we find that for $i = 1$ the element $D_{00}^1(1,2) = 0,\ D_{00}^1(1,2) = 0$ and all the others are arbitrary. One possible choice for the remaining elements is to

specify $A_j + D_{0j}^1 C = 0, j = 0, 1$. This choice results in the gain matrices:

$$D_0^1(\rho) = \begin{bmatrix} 2 & 0 \\ 0 & 0 \\ 0 & 0 \end{bmatrix}$$
$$D_0^2(\rho) = \begin{bmatrix} 0 & 0 \\ 0 & 1 \\ 0 & -0.5 \end{bmatrix} + \rho \begin{bmatrix} 0 & 0 \\ 0 & -\rho \\ 0 & -\rho \end{bmatrix}. \tag{38}$$

Having the parameter varying $D_0(\rho)$ calculated we need the output mixing H for which Ker $H_i C$ = Ker $C + \mathcal{S}_i^*$, $i = 1, 2$. Let V_i be a matrix for which ImV_i = Ker$C + \mathcal{S}_i^*$ and let the columns of $\overline{V}_i$ be basis in Ker V_i^T. Then for H_i we have

$$C^T H_i^T = \overline{V}_i. \tag{39}$$

It was supposed that C had full row rank, thus a possible choice for H is $H_i = ((CC^T)^{-1} C\overline{V_i})^T$. In our case

$$\overline{V}_1 = [0, 1, 0]^T; \qquad \overline{V}_2 = [1, 0, 0]^T. \tag{40}$$

and

$$H_1 = [0 \quad 1]; \qquad H_2 = [1 \quad 0]. \tag{41}$$

In the example we find that

$$M_1 = [1, 0], \qquad M_2 = 1. \tag{42}$$

The next step is to compute the restriction of the map $A_0(\rho) = (A(\rho) + D_0(\rho)C) \mid \mathcal{X}/\mathcal{S}^*$ using the formulae $P_i(A_j + D_{0j}^i C)P_i^T, i = 1, 2, j = 0, 1$.

Computation of the stabilizing gain $D_1^i(\rho) = D_{10} + \rho D_{11}^i, i = 1, 2$ will be performed using linear matrix inequalities (LMI). For simplicity the index i will be omitted, but

the subsequent LMI has to be solved for both detection filters.

We are looking for a positive definite X matrix and D_{10}, D_{11} for which

$$\begin{aligned} X &> 0 \\ (A_0(\rho) + D_1(\rho)M)^T X + X(A_0(\rho) + D_1(\rho)M) &< 0 \quad \forall \rho \in \mathcal{P}. \end{aligned} \tag{43}$$

Here $D_1(\rho) = D_{10} + \rho D_{11}$. It can be proved that for affine LPV systems the LMIs have to be solved only for the vertices of $\mathcal{P}$. Introducing the new variables:

$$K(\rho) := XD_1(\rho) = XD_{10} + \rho XD_{11} =: K_0 + \rho K_1, \tag{44}$$

the LMI variables are P which is symmetric positive definite and $K = [K_0, K_1]$ which is rectangular. Denote

$$M(\rho) = \begin{bmatrix} M \\ \rho M \end{bmatrix}. \tag{45}$$

Now the LMI to be solved is

$$A^T(\rho)X + XA(\rho) + M^T(\rho)K^T + KM(\rho) < 0 \tag{46}$$

for all $\rho \in \mathcal{P}_0$ which is a *feasibility problem.*

From the solution we obtain

$$\begin{aligned} D_1^1(\rho) &= \begin{bmatrix} 0.5593 \\ -1.0932 \end{bmatrix} + \rho \begin{bmatrix} -1 \\ -1 \end{bmatrix} \\ D_1^2(\rho) &= -1.5 \end{aligned} \tag{47}$$

Having the gains $D_0^i(\rho), D_1^i(\rho)$ and the matrices H_i, P_i one can compute the FDI matrices $N_i, G_i, F_i, i = 1, 2$. The complete filters in the example are:

$$\begin{aligned}
\dot{w}_1(t) = & \left(\begin{bmatrix} 0.5593 & 0.5000 \\ -1.0932 & -1.0000 \end{bmatrix} + \rho \cdot \begin{bmatrix} -1 & 0 \\ -1 & 0 \end{bmatrix} \right) \cdot w_1(t) \\
& - \left(\begin{bmatrix} 0.5593 & 0 \\ -1.0932 & 0 \end{bmatrix} + \rho \cdot \begin{bmatrix} -1 & 0 \\ -1 & 0 \end{bmatrix} \right) \cdot y(t) + \begin{bmatrix} 0 & 1 \\ 0 & 0 \end{bmatrix} \cdot u(t) \\
r_1(t) = & \begin{bmatrix} 1 & 0 \end{bmatrix} \cdot w_1(t) - \begin{bmatrix} 0 & 1 \end{bmatrix} \cdot y(t) \\
\dot{w}_2(t) = & -3.5 w_2(t) - \begin{bmatrix} 1.5 & 0 \end{bmatrix} \cdot y(t) + \begin{bmatrix} 1 & 0 \end{bmatrix} \cdot u(t) \\
r_2(t) = & \, w_2(t) - \begin{bmatrix} 1 & 0 \end{bmatrix} y(t).
\end{aligned} \tag{48}$$

B Appendix

In this appendix an example of the transformation from a nonlinear state equation to the affine LPV model required is shown in detail. The selected state is the angle of attack and the full nonlinear equation given in equation (49) is obtained from [20]:

$$\begin{aligned}
\dot{\alpha} = & \left[\, 1 - \frac{\bar{q} S \bar{c}}{2 m {V_T}^2} \, (1.45 - 1.8 \, x_{cg}) \, \frac{dC_L}{dq} \, \right] q + \left[\, - \frac{\bar{q} S}{m V_T} \, K_\alpha \, \frac{dC_L}{d\delta_e} \, \right] \delta_e \\
& + \left[\, - \frac{4}{m V_{TAS}} \, (s_\alpha + 0.0436 \, c_\alpha) \, \right] Tn + \frac{1}{V_{TAS}} \, (s_\alpha \, s_\theta + c_\alpha \, c_\theta) \, g \\
& - \frac{\bar{q} S}{m V_{TAS}} \, C_{L_{basic}}
\end{aligned} \tag{49}$$

We are interested in an affine LPV representation of the state equation with respect to the scheduling variables, ρ_i, and linear on the states, $x(t) = [\alpha, \; q, \; V_T, \; \theta, \; h_e]$, and control inputs, $u(t) = [\delta_e, \; \delta_{st}, \; Tn]$:

$$\dot{\alpha} = \; A(\rho) \, x(t) + B(\rho) \, u(t) \tag{50}$$

where $A(\rho)$ and $B(\rho)$ are given by equation (1).

The requirement of linear dependency on the states and the control inputs is easily checked since equation (49) is already written grouping terms together based on their linear dependency. It is observed that all equation terms except for the last two fulfill this linear dependency requirement. The easiest approach to solve this problem is to introduce a fictitious input, e.g. δ_{fic}, which multiplies the last two terms and enables equation (49) to be rewritten in the format of equation (50). The control input vector is given by $\hat{u}(t) = [\delta_e,\ \delta_{st},\ Tn,\ \delta_{fic}]^\top$. The fictitious input is held constant at 1 radians.

Table 1 provides the minimum and maximum values for the nine scheduling parameters for the longitudinal LPV model of the Boeing 747-100/200 aircraft.

number	**parameter**	**units**	**minimum val.**	**maximum val.**
ρ_1	$\bar{q}$	N/m^2	4.1039e+03	4.3577e+04
ρ_2	$\frac{\bar{q}}{V_T}$	$N{\cdot}s/m^3$	2.7360e+01	1.5563e+02
ρ_3	$\frac{1}{V_T}$	s/m	3.5714e-03	6.6667e-03
ρ_4	γ	radians	-3.4907e-01	3.4907e-01
ρ_5	$C_{L_{basic}}\ \frac{\bar{q}}{V_T}$	$N{\cdot}s/m^3$	5.3889e-01	1.7981e+02
ρ_6	$\frac{\partial C_L}{\partial \delta_{el}}\ \frac{\bar{q}}{V_T}$	$N{\cdot}s/m^3$	1.9611e-01	4.0034e-01
ρ_7	$C_{D_{Mach}}\ \bar{q}$	N/m^2	7.3702e+01	1.3503e+03
ρ_8	$\frac{\partial C_m}{\partial \delta_{el}}\ \bar{q}$	N/m^2	-4.4844e+02	-1.1638e+02
ρ_9	$C_{m_{basic}}\ \bar{q}$	N/m^2	-7.0123e+03	4.3577e+03

Table 1: Scheduling parameters table.

Several assumptions were made after analyzing average values of the equation terms in the face of scheduling parameters, states and control inputs variations:

$$a_1 \approx 1 - \frac{\bar{q} S \bar{c}}{2 m {V_T}^2}\ (1.45 - 1.8\ x_{cg})\ \frac{dC_L}{dq}; \qquad a_2 \approx\ -\frac{S}{m}\ K_\alpha;$$

$$a_3 \approx\ -\frac{4}{m}\ (s_\alpha + 0.0436\ c_\alpha); \qquad a_4 \approx (s_\alpha\ s_\theta + c_\alpha\ c_\theta)\ g;$$

$$a_5 \approx\ -\frac{S}{m};$$

where a_i represent constants values. Hence, equation (49) is rewritten as an affine LPV model:

$$\begin{aligned}\dot{\alpha} &= a_1\, q + a_2\, \rho_6\, \delta_e + a_3\, \rho_3\, Tn + a_4\, \rho_3\, \delta_{fic} + a_5\, \rho_5\, \delta_{fic} \\ &= \begin{bmatrix} 0 & a_1 & 0 & 0 & 0 \end{bmatrix} x(t) + \begin{bmatrix} a_2\, \rho_6 & 0 & a_3\, \rho_3 & (a_4\, \rho_3 + a_5\, \rho_5) \end{bmatrix} \hat{u}(t)\end{aligned} \tag{51}$$